

Phase-space representations of SIC-POVM fiducial states

Marcos Saraceno,^{1,2} Leonardo Ermann,^{1,3} and Cecilia Cormick⁴

¹*Departamento de Física Teórica, Comisión Nacional de Energía Atómica, Buenos Aires, Argentina*

²*Escuela de Ciencia y Tecnología, Universidad Nacional de San Martín, San Martín, Argentina*

³*CONICET, Godoy Cruz 2290 (C1425FQB) CABA, Argentina*

⁴*IFEG, CONICET and Universidad Nacional de Córdoba, Ciudad Universitaria, Córdoba, Argentina*

(Dated: December 8, 2016)

The problem of finding symmetric informationally complete POVMs (SIC-POVMs) has been solved numerically for all dimensions d up to 67 (A.J. Scott and M. Grassl, *J. Math. Phys.* 51:042203, 2010), but a general proof of existence is still lacking. For each dimension, it was shown that it is possible to find a SIC-POVM which is generated from a fiducial state upon application of the operators of the Heisenberg-Weyl group. We draw on the numerically determined fiducial states to study their phase-space features, as displayed by the characteristic function and the Wigner, Bargmann and Husimi representations, adapted to a Hilbert space of finite dimension. We analyze the phase-space localization of fiducial states, and observe that the SIC-POVM condition is equivalent to a maximal delocalization property. Finally, we explore the consequences in phase space of the conjectured Zauner symmetry. In particular, we construct an Hermitian operator commuting with this symmetry that leads to a representation of fiducial states in terms of eigenfunctions with definite semiclassical features.

PACS numbers:

I. INTRODUCTION

The question of the existence of symmetric informationally complete positive-operator valued measures (SIC-POVMs) [1–4] can be mapped to a variety of equivalent problems which have been investigated for many years eluding a conclusive answer. Initially posed as a mathematical problem of finding equiangular lines [5], this line of research has recently attracted renewed attention due to its relevance for quantum state tomography [6, 7] and quantum cryptography [8].

In his PhD thesis [1], G. Zauner conjectured that for any Hilbert-space dimension d a solution exists which is generated by the Heisenberg-Weyl group acting on a *fiducial state*, and which has a certain additional symmetry under a unitary operator. The name SIC-POVM was introduced in [2], which provided analytical solutions for d up to 4 and numerical solutions for d up to 45. The case of non-prime-power dimension 6 was studied in detail in [9], and general covariance properties were analyzed in [3] and [10]. In [4], the relevance of SIC-POVMs for quantum state tomography was highlighted, showing the optimality of this choice under statistical errors. The connection between SIC-POVMs and discrete Wigner functions [11] was explored first in [12], and later on in a generalization of the problem in [13]. The work [14] focused on the importance of SIC-POVMs from a foundational point of view concerning the structure of Hilbert space, while the relation between SIC-POVMs and mutually unbiased bases was analyzed in [15] for prime dimensions. A recent computer study was reported in [16], including numerical solutions up to $d = 67$, together with some new analytical solutions.

The present work undertakes a new analysis of the problem from the viewpoint of phase-space represen-

tations. We consider the phase-space descriptions of SIC-POVM fiducial states, that is, the states that are used to generate the full POVM by application of the Heisenberg-Weyl group operators. In particular, we explore chord, Wigner-Weyl, Husimi and Bargmann representations, and show how the SIC-POVM conditions manifest in phase-space. Finally, we explore the phase-space localization properties of fiducial states. While our study does not lead to an answer of the problem, we hope that it can provide inspiration and new insights in the search for solutions.

This article is organized as follows: in Section II we give general definitions concerning SIC-POVMs and covariance under the Heisenberg-Weyl group. Section III is devoted to a review of different phase-space representations of quantum states in a Hilbert space of finite dimension d , providing examples of the application of such representations to particular fiducial states. In Section IV we study the localization properties of fiducial states through their inverse participation ratio in phase space. In Section V we consider a special symmetry conjectured by G. Zauner for SIC-POVMs in all dimensions [1] and analyze its classical counterpart. We show that a Hermitian operator commuting with the Zauner symmetry can be constructed, which is a variant of the Harper Hamiltonian and provides a basis to expand the fiducial states. This basis has characteristic classical and semiclassical ($d \rightarrow \infty$) features. Finally, Section VI summarizes our results. In the appendices we provide additional details of our calculations. For simplicity, we restrict to the simpler case of odd dimensions, so that phase-space representations are not redundant [11, 17].

II. SYMMETRIC INFORMATIONALLY COMPLETE POSITIVE-OPERATOR VALUED MEASURES

A. Definitions

From now on we address only scenarios with a finite Hilbert space of dimension d . A generalized measurement in quantum mechanics can be described as a *positive-operator valued measure* (POVM), and requires a set of positive operators \hat{M}_j , $j = 1, \dots, m$ fulfilling $\sum_j \hat{M}_j = \hat{\mathbb{I}}$. Such a measurement can always be cast as a projective von-Neumann measure in a larger Hilbert space [18]. A set of d^2 operators \hat{M}_j with the additional requirement of linear independence, $\det(A) \neq 0$ with $A_{jk} = \text{tr}(\hat{M}_j \hat{M}_k)$, allows one to fully reconstruct the state $\hat{\rho}$ from the measured values $p_j = \text{tr}(\hat{M}_j \hat{\rho})$. The operators are then said to form an *informationally complete POVM* (IC-POVM) [19].

A further requirement that the operators be proportional to one-dimensional projectors with uniform overlap yields

$$\hat{M}_j = \frac{1}{d} |\phi_j\rangle\langle\phi_j| \quad (1)$$

with

$$|\langle\phi_j|\phi_k\rangle|^2 = \frac{d\delta_{jk} + 1}{d + 1} \quad (2)$$

and the set is then referred to as a *symmetric IC-POVM* (SIC-POVM) [2].

It is not known whether it is possible, for an arbitrary finite dimension d , to find d^2 states $|\phi_j\rangle$ such that the projectors $|\phi_j\rangle\langle\phi_j|$ conform a SIC-POVM. The problem consists of $d^2(d^2 - 1)/2$ conditions on $d^2(d - 1)$ complex coefficients, which makes it overdetermined so that it may not always have a solution. Numerical or analytical solutions have been found for all $d = 2, 3 \dots 67$, and it is generally believed that a solution can always be found [1, 2, 16].

The problem has several other facets that make it interesting in other fields [2, 16]:

- A SIC-POVM is a set of d^2 equiangular lines in complex space \mathbb{C}^d .
- A SIC-POVM is a minimal 2-design, allowing one to compute averages over the Haar measure with finite sums.
- A SIC-POVM is a maximally equiangular tight frame.

Furthermore, SIC-POVMs are specially relevant for quantum state tomography due to their robustness against statistical errors [4].

B. Group-covariant SIC-POVMs and the Heisenberg-Weyl group

Within the available tools, the simplest and most efficient way to construct a SIC-POVM is to impose that the operators forming it can be obtained by the action of a group of unitary operators acting on a fiducial state $|\phi\rangle$ according to:

$$\hat{M}_j = \hat{U}_j |\phi\rangle\langle\phi| \hat{U}_j^\dagger, \quad j = 0, \dots, d^2 - 1. \quad (3)$$

The easiest procedure, proposed in [2], is to choose as unitaries U_j the discrete phase-space displacement operators \hat{T}_α of the Heisenberg-Weyl group [20, 21]. These displacement operators are defined for pairs of integers $\alpha = (\alpha_1, \alpha_2) \in \mathbb{Z}_d^2$, so that α_1 and α_2 are interpreted as the magnitudes of the displacement in position and momentum respectively. In terms of the operators \hat{T}_α , the SIC-POVM condition takes the form:

$$|\langle\phi|\hat{T}_\alpha|\phi\rangle|^2 = \frac{1}{d+1} \quad \forall \hat{T}_\alpha \neq \mathbb{I}. \quad (4)$$

We note that:

$$|\langle\phi|\hat{T}_\alpha|\phi\rangle|^2 = \text{tr}[\hat{\rho}(\hat{T}_\alpha \hat{\rho} \hat{T}_\alpha^\dagger)] \quad (5)$$

with $\hat{\rho} = |\phi\rangle\langle\phi|$, so that the SIC-POVM condition is a requirement on the correlation between $\hat{\rho}$ and its translated image. This correlation must be constant for all translations that are not equivalent to the identity. Fiducial states that satisfy it have been found algebraically for some values of d and numerically for all values $2 \leq d \leq 67$. The main purpose of this work is to explore the features of these states and their symmetries when they are displayed in phase space.

We now review the definitions and main properties of the displacement operators and also of the reflection operators that provide the Wigner-Weyl representation of quantum mechanics. In the discrete case, one considers the vectors of an orthonormal basis $\{|n\rangle, n = 0, 1, \dots, d - 1\}$ as discretized position eigenstates with periodic boundary conditions, and their Fourier transforms $\{|k\rangle, k = 0, 1, \dots, d - 1\}$ as discretized momentum states. The elements of the two bases are related by $\langle k|n\rangle = \exp(-2\pi i kn/d)$. The Schwinger operators \hat{V} , \hat{U} implement the basic position and momentum translations as:

$$\hat{V}|n\rangle = |n + 1 \pmod{d}\rangle \quad (6)$$

$$\hat{U}|n\rangle = \omega^n |n\rangle \quad (7)$$

where

$$\omega = \exp(2\pi i/d) \quad (8)$$

is a d -root of unity. By definition, \hat{U} and \hat{V} satisfy $\hat{U}^d = \hat{V}^d = \hat{\mathbb{I}}$. Displacement operators are then defined for all pairs of integers $\alpha = (\alpha_1, \alpha_2) \in \mathbb{Z}^2$ as

$$\hat{T}_\alpha = \hat{V}^{\alpha_1} \hat{U}^{\alpha_2} \tau^{\alpha_1 \alpha_2}, \quad (9)$$

where

$$\tau = e^{i\pi(d+1)/d}. \quad (10)$$

For the phases we have adopted the notation of [3] that allows one to neatly separate the even and odd d cases. Some convenient properties of this definition are $\omega = \tau^2$, $\tau^{2d} = \tau^{d^2} = 1$, valid for all d .

\hat{T}_α is the (projective) unitary representation in the Hilbert space \mathcal{H}_d of the group of discrete phase-space translations with coordinates $\alpha = (\alpha_1, \alpha_2)$. The operators satisfy the properties:

$$\hat{T}_\alpha^\dagger = \hat{T}_{-\alpha}, \quad (11)$$

$$\hat{T}_\alpha \hat{T}_\beta = \tau^{\langle \alpha, \beta \rangle} \hat{T}_{\alpha+\beta}, \quad (12)$$

where the symplectic product $\langle \alpha, \beta \rangle$ is defined as:

$$\langle \alpha, \beta \rangle = \alpha_2 \beta_1 - \alpha_1 \beta_2 = -\langle \beta, \alpha \rangle. \quad (13)$$

The additional property

$$\hat{T}_{\alpha+d\beta} = \epsilon^{\langle \alpha, \beta \rangle} \hat{T}_\alpha, \quad (14)$$

with

$$\epsilon = \tau^d = \begin{cases} 1 & d \text{ odd} \\ -1 & d \text{ even} \end{cases} \quad (15)$$

means that the operators are periodic in the $d \times d$ lattice for odd d and in a $2d \times 2d$ lattice for even d .

In the following we treat explicitly the simpler case of odd d . In this case the division by two is unambiguously given by $2^{-1} \equiv \frac{1}{2} \pmod{d} = (d+1)/2$. One can then write $\tau = \omega^{\frac{1}{2}} \equiv \omega^{(d+1)/2}$, and rewrite \hat{T}_α as

$$\hat{T}_\alpha = \sum_{j \in \mathbb{Z}_d} |j + \alpha_1/2\rangle \langle j - \alpha_1/2| \omega^{\alpha_2 j}. \quad (16)$$

where all operations inside kets and bras are performed mod d . The d^2 operators are linearly independent and orthonormal under the trace product, namely, they satisfy:

$$\text{tr}(\hat{T}_\beta \hat{T}_\alpha^\dagger) = d \delta(\beta, \alpha). \quad (17)$$

The closely related reflection (or phase-space point) operators are defined by a symplectic Fourier transform of translations [11]:

$$\hat{R}_\mathbf{x} = \frac{1}{d} \sum_{\alpha \in \mathbb{Z}_d^2} \omega^{\langle \mathbf{x}, \alpha \rangle} \hat{T}_\alpha \quad (18)$$

with $\mathbf{x} \in \mathbb{Z}_d^2$. They are easily evaluated as

$$\hat{R}_\mathbf{x} = \sum_{j \in \mathbb{Z}_d} |x_1 + j/2\rangle \langle x_1 - j/2| \omega^{x_2 j}. \quad (19)$$

and inherit from the displacements the properties $\hat{R}_\mathbf{x} = \hat{R}_\mathbf{x}^\dagger$ and $\hat{R}_\mathbf{x}^2 = \hat{\mathbb{I}}$ so that they are both Hermitian and unitary. They are also linearly independent and orthogonal

$$\text{tr}(\hat{R}_\mathbf{x} \hat{R}_\mathbf{y}) = d \delta(\mathbf{x}, \mathbf{y}). \quad (20)$$

Special values of interest are

$$\hat{R}_{0,0} = \sum_{j \in \mathbb{Z}_d} |j\rangle \langle -j| = \frac{1}{d} \sum_{\alpha \in \mathbb{Z}_d^2} \hat{T}_\alpha, \quad (21)$$

$$\hat{T}_{0,0} = \sum_{j \in \mathbb{Z}_d} |j\rangle \langle j| = \frac{1}{d} \sum_{\mathbf{x} \in \mathbb{Z}_d^2} \hat{R}_\mathbf{x}. \quad (22)$$

III. PHASE-SPACE REPRESENTATIONS

The continuous group of Weyl displacements and the associated set of reflections have provided a way to express the quantum-mechanical treatment of a particle in one spatial dimension as a phase-space theory, but with the characteristic features due to the uncertainty principle exactly built in. Operators, observables and quantum states can be mapped under certain restrictions to c-number phase-space quasi-distributions and conversely functions in phase space can be quantized as operators in Hilbert space. In the discrete case an analogous situation arises [11, 17, 22, 23]. The two unitary bases described in the previous section provide a way to represent any operator in \mathcal{H}_d in terms of discrete c-number arrays with the properties of phase-space quasi-distributions. On the other hand continuous representations are also possible for operators in \mathcal{H}_d in terms of specially adapted Bargmann and Husimi functions [24–26]. In the following we review briefly the definitions and discuss the features displayed by these representations as they pertain to the structure of SIC-POVM fiducial states.

A. Discrete phase-space representations

Using the orthogonality condition (17), the d^2 linearly independent translations can be used as a basis to represent any operator \hat{A} as:

$$C_A(\alpha) = \text{tr}(\hat{A} \hat{T}_\alpha^\dagger) \quad (23)$$

where $\alpha = (\alpha_1, \alpha_2) \in \mathbb{Z}_d^2$. In terms of these coefficients the operator can be reconstructed as:

$$\hat{A} = \frac{1}{d} \sum_{\alpha \in \mathbb{Z}_d^2} C_A(\alpha) \hat{T}_\alpha \quad (24)$$

The same can be done in the reflection basis

$$W_A(\mathbf{x}) = \text{tr}(\hat{A} \hat{R}_\mathbf{x}) \quad (25)$$

and the reconstruction then reads

$$\hat{A} = \frac{1}{d} \sum_{\mathbf{x} \in \mathbb{Z}_d^2} W_A(\mathbf{x}) \hat{R}_\mathbf{x}. \quad (26)$$

$C_A(\alpha)$ is called the Weyl (or chord) representation of the operator, while $W_A(\mathbf{x})$ is its Wigner (or center) representation. The alternative names [27] arise from the

fact that the transformation $\mathbf{x}_A \mapsto \mathbf{x}_B$ is labeled by the chord $\boldsymbol{\alpha} = \mathbf{x}_B - \mathbf{x}_A$ in the case of translations, while for reflections it is labeled by the center $(\mathbf{x}_A + \mathbf{x}_B)/2$.

Standard properties of these representations are:

$$\text{tr}(\hat{A}) = C_A(0,0) = \frac{1}{d} \sum_{\mathbf{x} \in \mathbb{Z}_d^2} W_A(\mathbf{x}) \quad (27)$$

$$\text{tr}(\hat{A}\hat{B}) = \frac{1}{d} \sum_{\boldsymbol{\alpha} \in \mathbb{Z}_d^2} C_A(\boldsymbol{\alpha})C_B(-\boldsymbol{\alpha}) \quad (28)$$

$$= \frac{1}{d} \sum_{\mathbf{x} \in \mathbb{Z}_d^2} W_A(\mathbf{x})W_B(\mathbf{x}) \quad (29)$$

When applied to density matrices $\hat{\rho}$, $C_\rho(\boldsymbol{\alpha})$ is usually called the characteristic function while $W_\rho(\mathbf{x})$ is the Wigner function. However the standard normalization is different. For uniformity, we prefer to keep the normalization implied in (27). With this normalization the values of the Wigner or chord function of a normalized state ρ are bounded as $|C_\rho(\boldsymbol{\alpha})| \leq 1$ and $|W_\rho(\mathbf{x})| \leq 1$.

Furthermore, for a Hermitian operator $\hat{A} = \hat{A}^\dagger$, $W_A(\mathbf{x})$ is real and $C_A(\boldsymbol{\alpha}) = C_A(-\boldsymbol{\alpha})^*$, where $-\boldsymbol{\alpha}$ is understood to be taken modulo d . Other operator features are more difficult to write in terms of these representations, in particular positivity for a density operator or the pure-state condition $\hat{\rho}^2 = \hat{\rho}$. The latter leads to the non-linear relations:

$$C_\rho(\boldsymbol{\alpha}) = \frac{1}{d} \sum_{\boldsymbol{\beta} \in \mathbb{Z}_d^2} C_\rho(\boldsymbol{\beta})C_\rho(\boldsymbol{\alpha} - \boldsymbol{\beta})\tau^{\langle \boldsymbol{\alpha}, \boldsymbol{\beta} \rangle}, \quad (30)$$

$$W_\rho(\mathbf{x}) = \frac{1}{d^2} \sum_{\mathbf{x}_1, \mathbf{x}_2 \in \mathbb{Z}_d^2} W_\rho(\mathbf{x}_1)W_\rho(\mathbf{x}_2)\omega^{2\langle \mathbf{x} - \mathbf{x}_1, \mathbf{x} - \mathbf{x}_2 \rangle}. \quad (31)$$

The defining Eq. (4) for a SIC-POVM fiducial state imposes a necessary structure for its chord representation. Thus a putative SIC-POVM fiducial state must be of the form:

$$\hat{\sigma} = \frac{1}{d} \left[\hat{\mathbb{I}} + \frac{1}{\sqrt{d+1}} \sum_{\boldsymbol{\alpha} \neq 0} e^{i\psi_\alpha} \hat{T}_\alpha \right]. \quad (32)$$

If the phases ψ_α are chosen to satisfy $\psi_\alpha = -\psi_{-\alpha}$, then $\hat{\sigma}$ is Hermitian and $\text{tr} \hat{\sigma}^2 = \text{tr} \hat{\sigma} = 1$. However, the resulting operator is not necessarily positive. Enforcing the non-linear condition (30) that makes $\hat{\sigma}$ a pure state shows the difficulty of characterizing (and finding) fiducial states.

In Fig. 1 we show as an example the chord and Wigner representations of a fiducial state for the case $d = 5$ (the state coefficients are taken from [16], where the state is labeled “5a”). Each square in the figure represents the value of ψ_α in the region $-(d-1)/2 \leq \alpha \leq (d-1)/2$ for the chord function and the real values of the Wigner function $W_\rho(\mathbf{x})$ in $-(d-1)/2 \leq \mathbf{x} \leq (d-1)/2$. The triangles

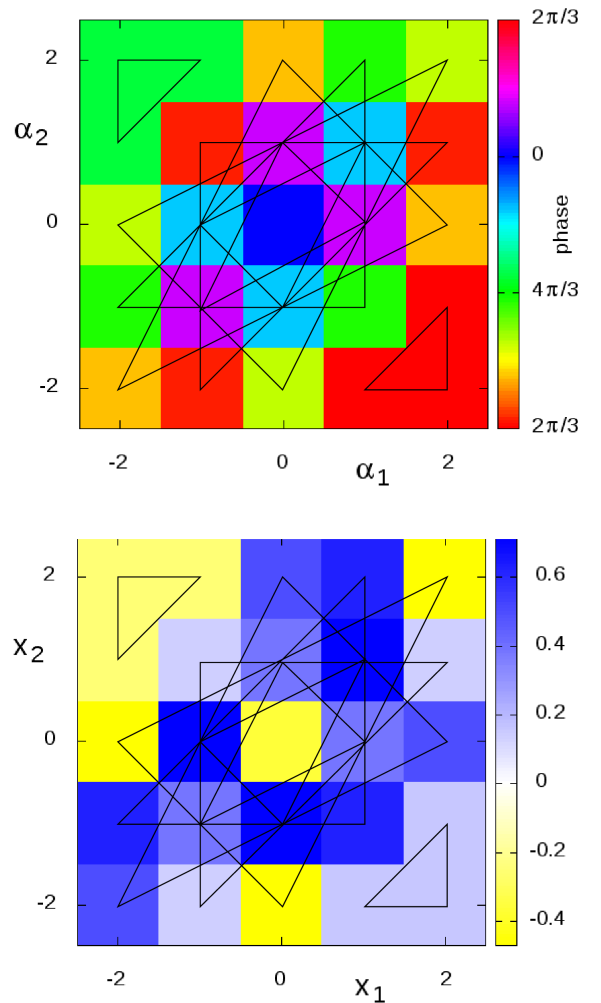


FIG. 1: (color online) Chord and Wigner representations of the state “5a” in the list in [16] in top and bottom panels respectively. The color scheme adopted is HLS, with hue and lightness labeling phase and modulus. In the bottom figure blue is positive and yellow negative. The triangles indicate the cycles of period three of the Zauner map, connecting equal values of the distributions. (see Sec. V).

connect equal values of the distributions on the cycles of the Zauner map (see Sec.V) displaying the Zauner symmetry of the state. Notice that $W_\rho(\mathbf{x})$ was computed for this state in [12].

B. Husimi and Bargmann representations

The Bargmann representation of quantum mechanics [28] maps the Hilbert space of square integrable functions on the real line to one of analytic (entire) functions in the complex plane. Namely, the Bargmann transform of a state $|\psi\rangle$, $\psi(z) = \langle z|\psi\rangle$, is given by its projection over the coherent states $|z\rangle$, $z \in \mathbb{C}$ with $z = q - ip$, each of which is an unnormalized Gaussian wave-packet centered

at the phase-space point $\{q, p\}$. The kernel that provides the mapping for the position kets $|x\rangle, x \in \mathbb{R}$ is:

$$\langle z|x\rangle = \frac{1}{(\pi\hbar)^{\frac{1}{4}}} \exp\left\{\frac{1}{\hbar}\left[-\frac{(z-x)^2}{2} + \frac{z^2}{4}\right]\right\}. \quad (33)$$

Here, \hbar is left explicitly as a dimensionless measure of the elementary quantum cell in phase space.

The Husimi representation of the state is closely related with the Bargmann representation and is given by the expression:

$$H_\psi(z, \bar{z}) \equiv H_\psi(q, p) = \frac{|\langle z|\psi\rangle|^2}{\langle z|z\rangle} = |\langle z|\psi\rangle|^2 e^{-|z|^2/(2\hbar)} \quad (34)$$

where the overline stands for complex conjugation. As opposed to the Wigner function, which cannot be interpreted as a probability distribution because it can take negative values, the Husimi representation is clearly positive by construction.

The adaptation of the Bargmann representation to \mathcal{H}_d with a phase space with periodic boundary conditions in position and momentum [24] (a unit torus) entails the immediate consequence that \hbar can only take the values

$$\hbar^{-1} = 2\pi d \quad (35)$$

so that the unit torus is spanned by d quantum states of area $2\pi\hbar$. Moreover position and momentum eigenstates are discretized as $|x\rangle \rightarrow |n/d\rangle, n \in \mathbb{Z}_d$ and $|p\rangle \rightarrow |k/d\rangle, k \in \mathbb{Z}_d$. To complete the construction the kernel is imposed to be periodic on the interval $0 \leq x \leq 1$ resulting in the definition

$$\langle z|n/d\rangle_d = \sum_{\mu \in \mathbb{Z}} \langle z|n/d + \mu\rangle. \quad (36)$$

Using (33) we obtain

$$\langle z|n/d\rangle_d = \exp\left\{2\pi d \left[\frac{z^2}{4} - \frac{(z - n/d)^2}{2}\right]\right\} \theta_3(i\pi(n - dz)|id) \quad (37)$$

Where θ_3 is the Jacobi theta function with the convention from [29]:

$$\theta_3(z|\tau) = \sum_{\mu \in \mathbb{Z}} e^{i\pi\tau\mu^2} e^{2i\mu z} \quad (38)$$

With this definition any state $|\psi\rangle$ in \mathcal{H}_d with coefficients $\langle n|\psi\rangle$ is mapped to the Bargmann function in the form:

$$B_\psi(z) = \langle z|\psi\rangle_d = \sum_{n \in \mathbb{Z}_d} \langle z|n/d\rangle_d \langle n|\psi\rangle \quad (39)$$

According to this mapping, $\langle z|\psi\rangle_d$ is an entire analytic function which moreover satisfies the following quasiperiodic boundary conditions in the fundamental unit cell in \mathbb{C} [24]:

$$\begin{aligned} \langle z+1|\psi\rangle_d &= e^{\pi d(\frac{1}{2}+z)} \langle z|\psi\rangle_d, \\ \langle z+i|\psi\rangle_d &= e^{\pi d(\frac{1}{2}-iz)} \langle z|\psi\rangle_d. \end{aligned} \quad (40)$$

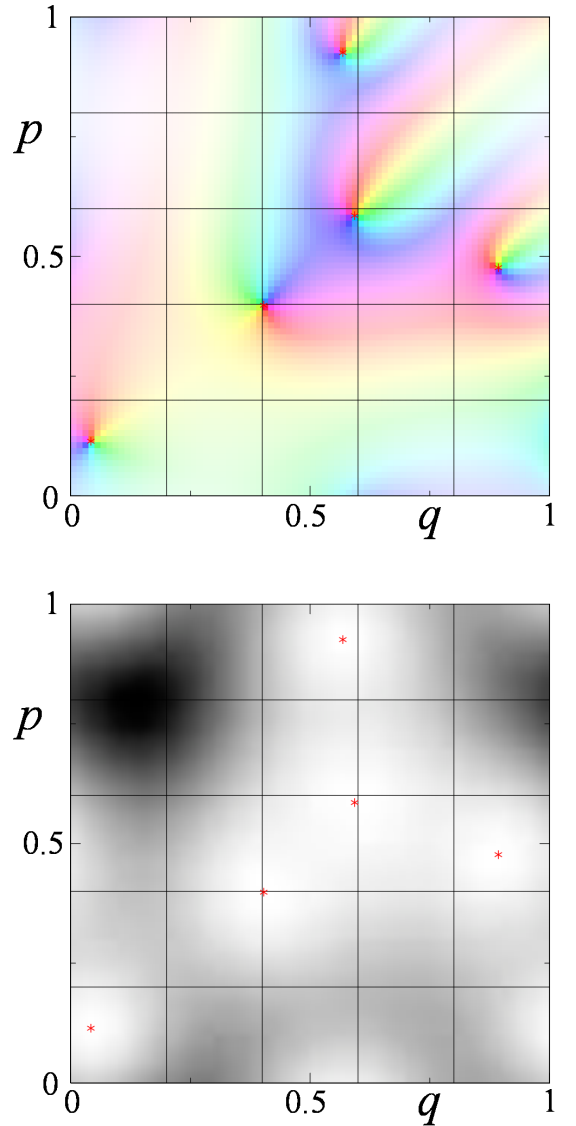


FIG. 2: (color online) The Husimi and Bargmann representation of the state “5a” in the list in [16]. The bottom panel represents the Husimi density, Eq. (34) with a linear intensity scale between the maximum and zero. The locations of the 5 zeroes are also marked. The top panel displays the phase of the Bargmann function, Eq. (39), in the fundamental cell. The zeroes are located at the phase dislocations.

Using Cauchy’s theorem and these boundary conditions to integrate on the contour of the unit cell, it is easy to show that there are exactly d zeroes in it and this pattern of zeroes is periodically repeated in the whole complex plane. The zeroes $z_i, i = 1, \dots, d$ in the unit cell are constrained by the relation

$$\frac{1}{d} \sum_{i=1}^d z_i = \frac{(1+i)}{2} \pmod{(1, i)} \quad (41)$$

Knowledge of the zeroes enables the full reconstruction of the quantum state via the Hadamard factorization of

entire functions, which in our case becomes

$$\langle z|\psi\rangle_d = C(z) \prod_{i=1}^d \langle z + z_0 - z_i|0\rangle_1 \quad (42)$$

Where $C(z)$ is non-vanishing and the factors are the fundamental quasi-periodic functions for $d = 1$:

$$\langle z|0\rangle_1 \equiv \psi_1(z) = e^{-\pi \frac{z^2}{2}} \theta_3(-i\pi z|i) \quad (43)$$

which have a single zero at $z_0 = (1+i)/2$ and are peaked at $z = 0$. The consequence is then that there is a one to one correspondence between the d complex zeroes constrained by Eq. (41) and the $d - 1$ complex amplitudes that define the normalized projector $|\psi\rangle\langle\psi|$. This highly non-linear correspondence, analogous to the relationship between the coefficients and the zeroes of a polynomial, constitutes the *stellar* representation of the pure state [24, 26].

The Husimi function, now defined as

$$H_\psi(z, \bar{z}) \equiv H_\psi(q, p) = |\langle z|\psi\rangle_d|^2 e^{-\pi d z \bar{z}}, \quad (44)$$

is positive and strictly periodic because of (40). The important observation [24] is that for pure states, this distribution inherits the zeroes of the Bargmann function and thus vanishes exactly at d points. It factorizes into products of elementary Husimi functions

$$H_\psi(z, \bar{z}) = \prod_{i=1}^d e^{-\pi z \bar{z}} |\theta_3(-i\pi(z + z_0 - z_i)|i)|^2. \quad (45)$$

In contrast with the Wigner and chord distributions, the pure state condition for the Husimi function is easily represented by this factorization formula, which does not hold for mixed states. Thus, a given pure state is uniquely defined by the distribution of d zeroes in the unit cell, constrained by having their center of mass in the center of the cell, Eq. (41). Understanding the special relations among the positions of these zeroes that make $|\psi\rangle$ a fiducial state is another way of stating the difficulty of the SIC-POVM problem.

As an illustration, Fig. 2 shows the Bargmann and Husimi representations of the state “5a” in the list in [16] (the same state whose Wigner and chord representations are given in Fig. 1). The zeroes of the Husimi density (bottom panel) can be identified as dislocations in the phase of the Bargmann function (top panel).

Husimi, chord and Wigner representation for odd-dimensional states up to $d = 67$ are available online at [30].

IV. LOCALIZATION MEASURES

In this section we use the fact that a SIC-POVM set is a two-design [31] to study the localization properties of fiducial states. We take as a measure of localization

the inverse participation ratio, which gives an idea of how “concentrated” a normalized probability distribution p_i , $i = 1 \cdots K$ is in its probability space. It is defined as:

$$P = \sum_{i=1}^K p_i^2. \quad (46)$$

For a normalized pure state $|\psi\rangle \in \mathcal{H}_d$ it takes the form

$$P_\psi = \sum_{i=0}^{d-1} |\langle i|\psi\rangle|^4 \quad (47)$$

Its value ranges from $P = d^{-1}$ for a state uniformly spread out in the basis considered, with $|\langle i|\psi\rangle| = 1/\sqrt{d} \forall i$, to $P = 1$ for each of the basis states. This quantity is strongly dependent on the chosen basis and in general has no invariant significance under unitary transformations of the state.

The inverse participation ratio for a fiducial state $|\phi\rangle$ follows from the two-design property

$$\begin{aligned} & \frac{1}{d^2} \sum_{\alpha \in \mathbb{Z}_d^2} \langle \phi|\hat{T}_\alpha^\dagger \hat{A}_1 \hat{T}_\alpha|\phi\rangle \langle \phi|\hat{T}_\alpha^\dagger \hat{A}_2 \hat{T}_\alpha|\phi\rangle \\ &= \int d\psi \langle \psi|\hat{A}_1|\psi\rangle \langle \psi|\hat{A}_2|\psi\rangle \end{aligned} \quad (48)$$

valid for arbitrary \hat{A}_1, \hat{A}_2 . The integral on the r.h.s. is over the normalized Haar measure and can be evaluated as [32, 33]:

$$\int d\psi \langle \psi|\hat{A}_1|\psi\rangle \langle \psi|\hat{A}_2|\psi\rangle = \frac{\text{tr}(\hat{A}_1 \hat{A}_2) + \text{tr}(\hat{A}_1) \text{tr}(\hat{A}_2)}{d(d+1)} \quad (49)$$

Replacing $\hat{A}_1 = \hat{A}_2 = |i\rangle\langle i|$ with $|i\rangle$ any of the basis states and combining (48) and (49) one obtains:

$$\frac{1}{d^2} \sum_{\alpha \in \mathbb{Z}_d^2} |\langle i|\hat{T}_\alpha|\phi\rangle|^4 = \frac{2}{d(d+1)} \quad (50)$$

which directly shows that:

$$P_{\text{SICPOVM}} = \sum_{i=0}^{d-1} |\langle i|\phi\rangle|^4 = \frac{2}{d+1}. \quad (51)$$

This result is the same in all other bases related by Clifford operations.

Making the same replacement in (49) one also sees that

$$\int d\psi |\langle i|\psi\rangle|^4 = \frac{2}{d(d+1)}, \quad (52)$$

which also implies:

$$\langle P \rangle_{\text{Haar}} = \int d\psi \sum_{i=0}^{d-1} |\langle i|\psi\rangle|^4 = \frac{2}{d+1}. \quad (53)$$

This means that the average value of the inverse participation ratio over random states distributed over the Haar measure is the same as its value for SIC-POVM fiducial states, with a localization half way between maximum and minimum. This is illustrated in Fig. 3 (top), which shows the degree of delocalization for different kinds of pure quantum states; for the sake of clarity we plot P^{-1} , a quantity that ranges between 1 and d , instead of P .

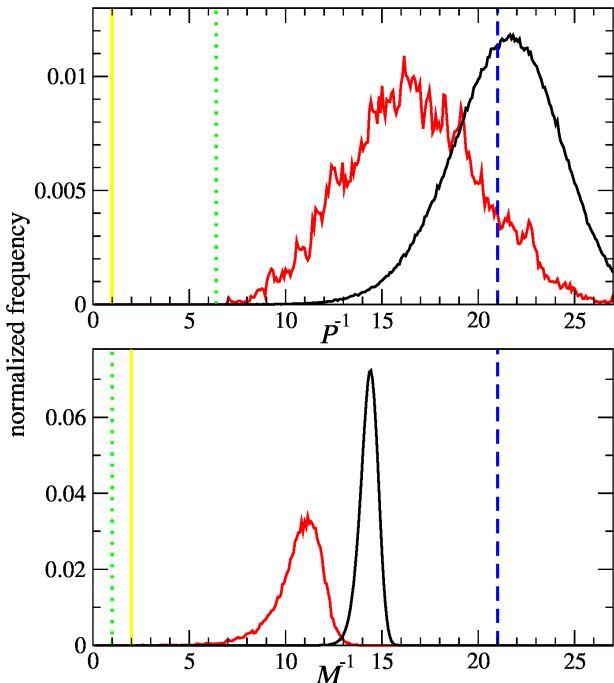


FIG. 3: (color online) Measures of delocalization for different quantum states for a Hilbert space of dimension $d = 41$. The top shows P^{-1} , with P the inverse participation ratio defined in Eq. (47), and the bottom panel the phase-space delocalization measure M^{-1} , with M from Eq. (54). The solid lines show the histograms for 10^6 random pure states (black), and eigenstates of a chaotic Harper map (red) with 500 bins in P^{-1} , $M \in [0, 41]$. Position, coherent and SIC-POVM fiducial states are represented in solid yellow, dotted green and dashed blue vertical lines respectively.

We now want to extend these considerations to phase-space localization. For the study of SIC-POVM fiducial states, we would like to define localization measures that share the invariance under Clifford operations. To this end we consider first the chord distribution, as defined in Eqs. (23-24). For a pure state, the condition $\text{tr}(\rho^2) = 1$ leads to the normalization $1/d \sum_{\alpha} |C(\alpha)|^2 = 1$. A suitable phase-space measure for localization can then take the form:

$$M_{\psi} = \frac{1}{d} \sum_{\alpha \in \mathbb{Z}_d^2} |C_{\psi}(\alpha)|^4 = \frac{1}{d} \sum_{\alpha \in \mathbb{Z}_d^2} |\langle \psi | \hat{T}_{\alpha} | \psi \rangle|^4. \quad (54)$$

In the same vein we can also consider the Wigner local-

ization as:

$$M_{\psi} = \frac{1}{d} \sum_{\alpha \in \mathbb{Z}_d^2} W_{\psi}^4(\mathbf{x}) = \frac{1}{d} \sum_{\alpha \in \mathbb{Z}_d^2} \langle \psi | \hat{R}_{\mathbf{x}} | \psi \rangle^4. \quad (55)$$

In Appendix A we show that, for pure states, these two definitions indeed coincide; besides, the covariance of \hat{T}_{α} and $\hat{R}_{\mathbf{x}}$ under Clifford operations shows that M is invariant under them as desired. M satisfies the bounds

$$\frac{2}{d+1} \leq M \leq 1. \quad (56)$$

The upper bound is a simple consequence of the fact that $|\langle \psi | \hat{T}_{\alpha} | \psi \rangle| \leq 1$ and is saturated, i.e., by position states $|\psi\rangle = |i\rangle$. The lower bound is more subtle [34] and the important result is that it is attained if and only if $|\psi\rangle$ is a fiducial state [2]. In fact M , written in a slightly different fashion, is the cost function used for numerical searches [16]. Thus, with respect to this measure of phase-space localization, we can identify SIC-POVM fiducial states as those maximally delocalized in phase space.

The Haar average of M can also be computed with the techniques of [35] with the result:

$$\langle M \rangle_{Haar} = \int d\psi M_{\psi} = \frac{3}{d+2} \quad (57)$$

(more details are given in Appendix B). So the phase-space localization properties of random states are clearly different from those of SIC-POVM fiducial states, in contrast to the behavior observed for localization in a given basis of the Hilbert space. The phase-space localization properties of different states are compared in Fig. 3 (bottom panel), where for clarity we plot M^{-1} instead of M .

V. THE ZAUNER SYMMETRY

A. Zauner operator and its classical counterpart

In his Ph.D. thesis [1], Zauner conjectured that the fiducial state of a Heisenberg-Weyl SIC-POVM was to be found as a particular eigenfunction of a unitary map. In the position representation, the map has the following matrix elements

$$\langle k | \hat{Z} | j \rangle = \frac{e^{i\chi}}{\sqrt{d}} \tau^{2kj+k^2} \quad (58)$$

Choosing the phase $\chi = \pi(d-1)/12$ the map has the property $\hat{Z}^3 = 1$. Its eigenvalues are thus $e^{i2\pi n/3}$ ($n = 0, 1, 2$) and the spectrum is highly degenerate for all large values of d . Because of the large degeneracy, the Zauner hypothesis puts a restriction on the fiducial state but by no means determines it completely. Finding a fiducial state can thus be considered as the numerical task of finding the particular linear combination of eigenstates of the Zauner map within one of its three multiplets and

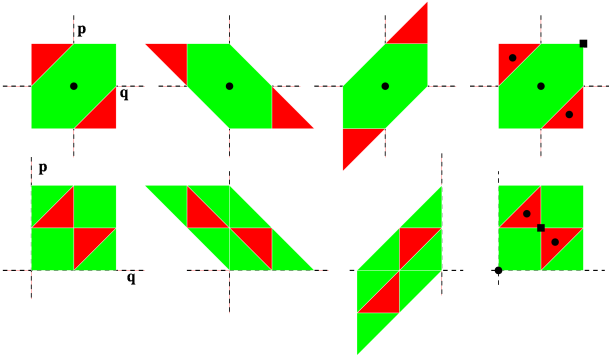


FIG. 4: Classical Zauner map representation in phase space. Invariant regions are shown in colors with fixed points represented by black dots. The top and bottom rows represent the action of the map for two equivalent choices of the phase space where origin is on the center and left bottom respectively.

satisfying Eq. (4). The map has two symmetries: a unitary symmetry under parity and an antiunitary one under time reversal. These are reflected in the properties

$$\hat{R}_0 \hat{Z} \hat{R}_0 = \hat{Z}, \quad \hat{F} \hat{Z} \hat{F}^\dagger = (\hat{Z}^*)^{-1} \quad (59)$$

where the asterisk denotes complex conjugation and \hat{F} is the Fourier operator $\langle i | \hat{F} | j \rangle = \omega^{-ij} / \sqrt{d}$.

The Zauner operator can be considered as the quantum version of a classical map which is a symplectic automorphism of a 2D torus. The map is defined on the square $E = [-\frac{1}{2}, \frac{1}{2}] \times [-\frac{1}{2}, \frac{1}{2}]$ and maps $(q, p) \in E$ to $(q', p') \in E$ according to:

$$q' = -p \quad (60)$$

$$p' = q - p - [2(q - p)] \quad (61)$$

where $[\cdot]$ denotes the integer part. It is an area-preserving elliptic “cat map” which is locally a composition of a negative shear followed by a $\pi/2$ rotation as illustrated in Fig. 4.

The map has three invariant regions E_0, E_1, E_{-1} which are determined by the value of $\epsilon = [2(p - q)] = 0, 1, -1$. These regions are shown in Fig. 4; for clarity, in the bottom row we show the map acting on the square $[0, 1) \times [0, 1)$. All orbits are of period three and their respective cycles are

$$\begin{pmatrix} q \\ p \end{pmatrix} \rightarrow \begin{pmatrix} -p \\ q - p - \epsilon \end{pmatrix} \rightarrow \begin{pmatrix} p - q + \epsilon \\ -q \end{pmatrix} \rightarrow \begin{pmatrix} q \\ p \end{pmatrix} \quad (62)$$

There are three fixed points belonging to each of the invariant regions E_i : $z_0 = (0, 0)$, $z_1 = (1/3, -1/3)$, $z_{-1} = (-1/3, 1/3)$. Moreover, the point $(q, p) = (\frac{1}{2}, \frac{1}{2})$ can be assimilated to a hyperbolic point with $q = \frac{1}{2}$ and $p = \frac{1}{2}$ as stable and unstable manifolds. The respective areas of the invariant regions are $\mu(E_1) = \mu(E_{-1}) = 1/8$ and $\mu_0 = 3/4$, with a total unit area.

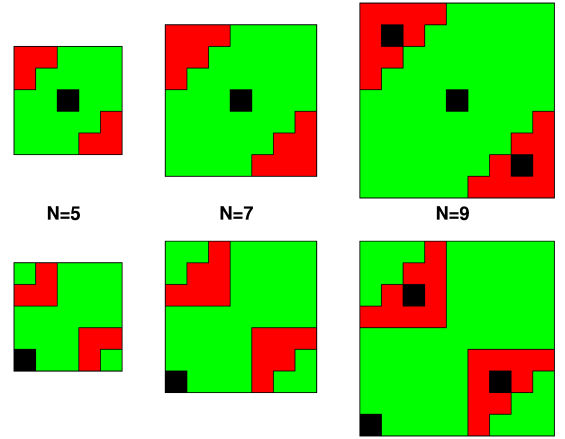


FIG. 5: Invariant regions for the discretized classical Zauner map. There are three fixed points if d is divisible by 3, and only one otherwise. As in the previous Figure, top and bottom rows correspond to two equivalent choices for the phase-space limits where origin is on the center and left bottom respectively.

The quantum Zauner map is a special Clifford operation that shares the basic property of mapping the Weyl operators among themselves, i.e.

$$\hat{Z} \hat{T}_\alpha \hat{Z}^\dagger = \hat{T}_{Z\alpha} \quad (63)$$

where Z is the discretized map acting as

$$Z\alpha = \begin{pmatrix} 0 & -1 \\ 1 & -1 \end{pmatrix} \begin{pmatrix} \alpha_1 \\ \alpha_2 \end{pmatrix} \pmod{d}. \quad (64)$$

The correspondence with the classical map is obtained discretizing $q, p \rightarrow \alpha_1/d, \alpha_2/d$ with

$$-(d-1)/2 \leq \alpha_1, \alpha_2 \leq (d-1)/2. \quad (65)$$

The invariant regions are preserved by the discretization and are now defined as \bar{E}_ϵ where $\epsilon = [2(\alpha_1 - \alpha_2)/d]$. The totality of d^2 points are divided in three invariant sets of dimension

$$\begin{aligned} \mu(\bar{E}_1) &= \mu(\bar{E}_{-1}) = \frac{(d-1)(d+1)}{8} \\ \mu(\bar{E}_0) &= d^2 - 2\frac{d^2-1}{8} = \frac{3d^2+1}{4} \end{aligned} \quad (66)$$

in close correspondence with the classical areas, if we assign to each point an area d^{-2} . We display the discrete invariant regions in Fig. 5. The fixed point at $\alpha = (0, 0)$ in the central region \bar{E}_0 survives the discretization for all odd d , while the other two fixed points only survive when d is an odd multiple of 3, and they occur at $\alpha_1 = (d/3, -d/3)$ and $\alpha_{-1} = (-d/3, d/3)$.

Taking into account that $Z^3 = 1$ we can divide each region into 3-cycles (and fixed points) as follows. It is easy to calculate the number N_i of 3-cycles in each region.

In \bar{E}_0 (excluding the trivial fixed point) the count is as follows:

$$N_0 = \frac{1}{3} \left(\frac{3d^2 + 1}{4} - 1 \right) = \frac{d^2 - 1}{4} \quad (67)$$

These cycles are further divided in two disjoint sets related by the symmetry $\alpha \rightarrow -\alpha$. In regions $\bar{E}_{\pm 1}$ the count depends on whether 3 divides d

$$N_{\pm 1} = \begin{cases} \frac{1}{3} \left(\frac{d^2 - 1}{8} - 1 \right) = \frac{d^2 - 9}{24} & \text{for } d/3 \text{ integer} \\ \frac{d^2 - 1}{24} & \text{otherwise} \end{cases} \quad (68)$$

These considerations are relevant for the structure of a fiducial state in the chord representation. In fact, the Zauner symmetry $\hat{Z}\hat{\sigma}\hat{Z}^\dagger = \hat{\sigma}$ imposed on Eq. (32) implies that the phases ψ_α must be constant along each of the 3-cycles. Then $\hat{\sigma}$ is further constrained as

$$\hat{\sigma} = \frac{1}{d} \left[\hat{1} + \frac{1}{\sqrt{d+1}} \sum_p \frac{e^{i\psi_p} \hat{M}_p + e^{-i\psi_p} \hat{M}_p^\dagger}{2} \right] \quad (69)$$

where p runs over all cycles other than the fixed point at the origin. In this expression we have explicitly used the phase relation between cycles reflected through the origin, and defined:

$$\hat{M}_p = \sum_{\alpha \in p} \hat{T}_\alpha. \quad (70)$$

Notice that each cycle can correspond to three points or only one, if d is divisible by 3. The total number of phases $\#p$ not constrained by the Zauner symmetry can be computed from Eqs. (67-68) and yield

$$\#p = \begin{cases} \frac{d^2 + 3}{6} & \text{for } d/3 \text{ integer} \\ \frac{d^2 - 1}{6} & \text{otherwise} \end{cases} \quad (71)$$

The analysis of the Wigner case proceeds in a similar way. Again the fact that $\hat{Z}\hat{R}_\mathbf{x}\hat{Z}^\dagger = \hat{R}_{Z\mathbf{x}}$ implies that the values of the Wigner function are constant on the cycles, although here there is no direct relationship between $W(\mathbf{x})$ and $W(-\mathbf{x})$. All these features are clearly seen in Fig.1, where we have marked the cycles joining equal values of the distributions.

B. Definition of a basis of eigenvectors of the Zauner map

To specify completely an eigenbasis of \hat{Z} one needs to find another operator commuting with it that can remove the degeneracies. We have constructed such an operator as a superposition of translations on one of the classical periodic orbits of Z :

$$\hat{H}^\alpha = \frac{1}{2} \left(\hat{T}_\alpha + \hat{T}_{Z\alpha} + \hat{T}_{Z^2\alpha} + \text{H.c.} \right). \quad (72)$$

The operator is labeled by one point on the orbit and is clearly Hermitian. Obviously $\hat{Z}\hat{H}^\alpha\hat{Z}^\dagger = \hat{H}^\alpha$. Moreover from the fact that $\hat{R}_0\hat{T}_\alpha\hat{R}_0 = \hat{T}_{-\alpha}$, \hat{H}^α also commutes with the parity operation. Thus the three commuting operators $\hat{Z}, \hat{H}^\alpha, \hat{R}_0$ have common eigenfunctions defined by the properties:

$$\hat{H}^\alpha |\psi_{ikr}\rangle = \epsilon_{ikr} |\psi_{ikr}\rangle \quad (73)$$

$$\hat{R}_0 |\psi_{ikr}\rangle = r |\psi_{ikr}\rangle \quad (74)$$

$$\hat{Z} |\psi_{ikr}\rangle = e^{2\pi i k/3} |\psi_{ikr}\rangle \quad (75)$$

where $r = \pm 1$, $k = 0, 1, 2$ and ϵ_{ikr} are the non-degenerate eigenvalues of \hat{H}^α .

We now take the simplest choice of such Hamiltonian, built on the orbit $(0, 1), (1, 0), (-1, -1)$ leading to

$$\hat{H} = \frac{\hat{U} + \hat{U}^\dagger}{2} + \frac{\hat{V} + \hat{V}^\dagger}{2} + \frac{\hat{U}\hat{V}\tau^* + \hat{V}^\dagger\hat{U}^\dagger\tau}{2}. \quad (76)$$

The resulting hermitian matrix is easily constructed and can be numerically diagonalized. In the limit of $d \rightarrow \infty$ it corresponds to the Weyl quantization of the classical Hamiltonian

$$H(q, p) = \cos(2\pi q) + \cos(2\pi p) - \cos[2\pi(q - p)]. \quad (77)$$

where $q, p \in [0, 1)$ are now continuous variables corresponding to $\alpha_1/d, \alpha_2/d$. This is a variant of the Harper Hamiltonian on the torus, in both its classical and quantum versions. In Fig. 6 we plot the level curves of $H(q, p)$, a smooth doubly periodic surface which displays very similar features as the map (cf. Fig. 5), sharing the invariant regions and the fixed points as critical points of the surface. The level curves $H(q, p) = E$ support semiclassically the eigenstates of the quantum Hamiltonian, with eigenvalues approximately quantized by the Bohr-Sommerfeld rule

$$S(E) = \oint_E p(E, q) dq = \frac{2\pi}{d} \left(i + \frac{1}{2} \right). \quad (78)$$

It is easy to check that the three points of each cycle of the classical map lie on one of these levels and each level supports a continuous family of such cycles.

In table I we show the numerically determined eigenvalues and quantum numbers of \hat{H} for $d = 7$. As an example, the fiducial state “7a” [16], which belongs to the multiplet $k = 0$, has the expansion

$$|7a\rangle = a_1 |\psi_{101}\rangle + a_5 |\psi_{50-1}\rangle + a_6 |\psi_{601}\rangle \quad (79)$$

where $a_1 \simeq 0.336$, $a_5 \simeq -0.691 + i0.230$, and $a_6 \simeq -0.107 + i0.587$. Thus, contrary to the representation in (69) in terms of classical cycles of the map, here the fiducial states are represented as superpositions of eigenfunctions of the quantum Hamiltonian, which have a clear semiclassical ($d \rightarrow \infty$) description in terms of “tori” of the classical Hamiltonian.

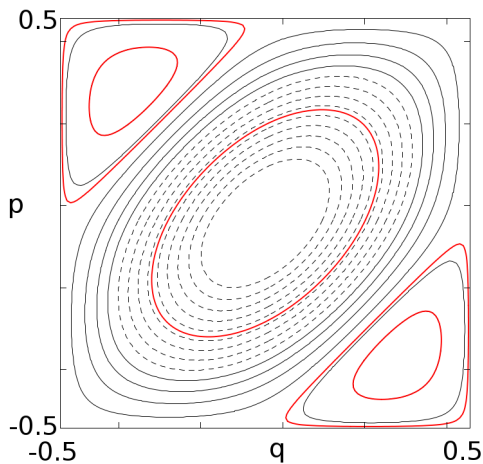


FIG. 6: (color online) Level curves for the classical Hamiltonian defined in Eq. (77). In boldface (red online) we display the three levels with energies that support the $k = 0$ symmetry for the state “7a”.

i	ϵ_i	r	k
0	-2.315069600541	-1	-1
1	-1.118527682059	1	0
2	-0.209389069220	-1	1
3	0.337407948091	1	-1
4	0.940071117953	1	1
5	1.024458669761	-1	0
6	1.341048616015	1	0

TABLE I: Eigenvalues of Hamiltonian \hat{H} from Eq. (76), and their corresponding quantum numbers r and k under parity and Zauner map respectively, for $d = 7$.

VI. CONCLUDING REMARKS

We have explored several ways of representing the fiducial states using phase-space methods. The discrete representations based on the chord and Wigner functions are very similar and (for odd d) yield $d \times d$ arrays respectively of phases with constant amplitudes or real (positive and negative) values. Clifford symmetries of the fiducial state thus represented are readily recognized because the array values are constant on the cycles of the classical symmetry. In particular, the presence of the Zauner symmetry organizes the distributions as superpositions of 3-cycles as in Eq. (69). However, the representation is highly redundant, as it depends on a number of parameters growing as d^2 , even taking into account the presence of symmetries, while the state itself only depends on $d - 1$ complex amplitudes. The imposition of the nonlinear pure-state condition directly in terms of these two quasidistributions remains elusive.

The continuum representation is much leaner, and in a way has complementary properties. The pure-state condition is readily accommodated by a constellation of $d - 1$ independent zeroes that parametrize the fiducial

state in a way equivalent to that provided by the representation in terms of amplitudes. However we have not found a clear signature in this constellation of the presence of a Clifford symmetry, besides of course the obvious invariance of the whole constellation. The reason is that, unlike what happens for the discrete representations, the zeroes do not “move” classically when the state is subjected to a Clifford operation. It remains also a major open issue to precisely formulate the fiducial SIC-POVM condition directly in terms of the zeroes of the constellation.

The fact that a SIC-POVM is a projective 2-design imposes some constraints on the localization properties of the fiducial states, as measured by the inverse participation ratio. When the fiducial state is expanded in the coordinate basis, its inverse participation ratio P has the same value as the average over random states. On the other hand, when fiducial states are described by means of the chord or the Wigner representations, the inverse participation ratio shows they are maximally delocalized in phase space, in contrast with the Haar average.

The conjectured Zauner symmetry shows up in interesting ways in the discrete representations, its main consequence being that the distributions become constant along the classical 3-cycles of the symmetry. The fiducial state is then represented as a superposition of the order of $(d^2 - 1)/3$ periodic cycles. In contrast, the representation as a superposition of the eigenstates of a Hamiltonian \hat{H} commuting with the Zauner operator, has the least possible freedom compatible with the symmetry ($\approx d/3$). Moreover the eigenstates retain simple semiclassical features that become sharper as $d \rightarrow \infty$.

In summary, we have explored various ways to display phase-space features of SIC-POVM fiducial states. Although none provides significant inroads to the deeper problem of the proof of existence, we present them in the hope that this study may illuminate from different angles some of the many facets of this most interesting problem.

Appendix A: Equivalence for pure states of the two definitions of the phase-space localization measure

To show that the two definitions of M in Eq. (54) are indeed equal we consider, for an arbitrary operator \hat{A} , the quantity

$$\text{tr}(\hat{R}_x \hat{A} \hat{R}_x \hat{A}) = \frac{1}{d^2} \sum_{\alpha, \beta} C_A(\alpha) C_A(\beta) \text{tr}(\hat{R}_x \hat{T}_\alpha \hat{R}_x \hat{T}_\beta) \quad (\text{A1})$$

where we have expanded \hat{A} in terms of the chord function using Eq. (24). Using the conjugation

$$\hat{R}_x \hat{T}_\alpha \hat{R}_x = \omega^{2\langle \alpha, x \rangle} \hat{T}_\alpha^\dagger \quad (\text{A2})$$

and the orthogonality of translations we deduce

$$\text{tr}(\hat{R}_x \hat{A} \hat{R}_x \hat{A}) = \frac{1}{d} \sum_{\alpha} C_A(\alpha) C_A(\alpha) \omega^{2\langle \alpha, x \rangle} \quad (\text{A3})$$

Now, if \hat{A} is a pure state $|\psi\rangle\langle\psi|$ the l.h.s. is the square of the Wigner function $W_\psi(\mathbf{x}) = \langle\psi|\hat{R}_\mathbf{x}|\psi\rangle$ and we have obtained

$$W_\psi(\mathbf{x})^2 = \frac{1}{d} \sum_{\alpha} \omega^{2\langle\alpha,\mathbf{x}\rangle} C_\psi(\alpha)^2 \quad (\text{A4})$$

Thus the square of the Wigner function is the symplectic Fourier transform of the square of the chord function. Parseval relation then immediately implies

$$\sum_{\mathbf{x}} W_\psi(\mathbf{x})^4 = \sum_{\alpha} |C_\psi(\alpha)|^4 \quad (\text{A5})$$

Appendix B: Averages over Haar measure

We are interested in averages of the type

$$\int d\psi \prod_{i=1}^t \langle\psi|\hat{A}_i|\psi\rangle \quad (\text{B1})$$

where the integration is over the complex projective space CP^{d-1} with the measure induced by the unitarily invariant Haar measure on $U(d)$. The symmetry of the integrand under the interchange of the \hat{A}_i turns this into a projector onto the totally symmetric subspace of the Hilbert space $\mathcal{H}^{\otimes t} \equiv C_d^{\otimes t}$ with dimension

$$D_t = \frac{(d+t-1)!}{(d-1)!t!} \quad (\text{B2})$$

The average can be expressed as a trace over permanents

$$\int d\psi \prod_{i=1}^t \langle\psi|\hat{A}_i|\psi\rangle = \frac{(d-1)!}{(d+t-1)!} \sum_{i_1 i_2 \dots i_t} \begin{vmatrix} \langle i_1|\hat{A}_1|i_1\rangle & \langle i_1|\hat{A}_2|i_2\rangle & \dots & \langle i_1|\hat{A}_t|i_t\rangle \\ \langle i_2|\hat{A}_1|i_1\rangle & \langle i_2|\hat{A}_2|i_2\rangle & \dots & \langle i_2|\hat{A}_t|i_t\rangle \\ \vdots & \vdots & \ddots & \vdots \\ \langle i_t|\hat{A}_1|i_1\rangle & \langle i_t|\hat{A}_2|i_2\rangle & \dots & \langle i_t|\hat{A}_t|i_t\rangle \end{vmatrix}_+ \quad (\text{B3})$$

The permanent can be evaluated in terms of all possible product of traces of the A_i . For $t=2$ and for traceless and unitary translations with $A_1 = A_2 = \hat{T}_\alpha, A_3 = A_4 = \hat{T}_\alpha^\dagger$, Eq. (B3) can be easily evaluated with the result:

$$\int d\psi \left| \langle\psi|\hat{T}_\alpha|\psi\rangle \right|^4 = \begin{cases} \frac{2}{(d+1)(d+2)} & \text{for } \alpha \neq 0 \\ 1 & \text{for } \alpha = 0 \end{cases} \quad (\text{B4})$$

Then we obtain Eq. (57)

$$\langle M \rangle_{Haar} = \frac{1}{d} \left\{ 1 + \frac{2(d^2-1)}{(d+1)(d+2)} \right\} = \frac{3}{d+2} \quad (\text{B5})$$

- [1] G. Zauner. Quantum designs: Foundations of a noncommutative design theory. *Int. J. Quant. Inf.*, 9:445, 2011. English translation of G. Zauner's Ph.D. Thesis (1999).
- [2] J. M. Renes, R. Blume-Kohout, A. J. Scott, and C. M. Caves. Symmetric informationally complete quantum measurements. *J. Math. Phys.*, 45:2171–2180, 2004.
- [3] D. M. Appleby. Symmetric informationally complete-positive operator valued measures and the extended Clifford group. *J. Math. Phys.*, 46:052107, 2005.
- [4] A. J. Scott. Tight informationally complete quantum measurements. *J. Phys. A: Math. Gen.*, 39:13507, 2006.
- [5] P. W. H. Lemmens and J. J. Seidel. Equiangular lines. *J. Algebra*, 24:494 – 512, 1973.
- [6] C. M. Caves, C. A. Fuchs, and R. Schack. Unknown quantum states: The quantum de Finetti representation. *J. Math. Phys.*, 43:4537–4559, 2002.
- [7] Z. E. D. Medendorp, F. A. Torres-Ruiz, L. K. Shalm,

- G. N. M. Tabia, C. A. Fuchs, and A. M. Steinberg. Experimental characterization of qutrits using symmetric informationally complete positive operator-valued measurements. *Phys. Rev. A*, 83:051801, 2011.
- [8] C. A. Fuchs and M. Sasaki. Squeezing quantum information through a classical channel: Measuring the “quantumness” of a set of quantum states. *Quantum Info. Comput.*, 3:377–404, 2003.
- [9] M. Grassl. On SIC-POVMs and MUBs in Dimension 6. e-print arXiv:quant-ph/0406175, 2004.
- [10] S. T. Flammia. On SIC-POVMs in prime dimensions. *J. Phys. A: Math. Gen.*, 39:13483–13493, 2006.
- [11] U. Leonhardt. Discrete wigner function and quantum-state tomography. *Phys. Rev. A*, 53:2998–3013, 1996.
- [12] S. Colin, J. Corbett, T. Durt, and D. Gross. About SIC-POVMs and discrete Wigner distributions. *J. Opt. B: Quant. Semiclass. Opt.*, 7:778, 2005.

- [13] D. M. Appleby. Symmetric informationally complete measurements of arbitrary rank. *Opt. Spect.*, 103:416–428, 2007.
- [14] D. M. Appleby, H. Bui Dang, and C. A. Fuchs. Symmetric informationally-complete quantum states as analogues to orthonormal bases and minimum-uncertainty states. e-print arXiv: 0707.2071, 2007.
- [15] D. M. Appleby. SIC-POVMS and MUBS: geometrical relationships in prime dimension. In L. Accardi, G. Adenier, C. Fuchs, G. Jaeger, A. Y. Khrennikov, J.-Å. Larsson, and S. Stenholm, editors, *American Institute of Physics Conference Series*, volume 1101 of *American Institute of Physics Conference Series*, pages 223–232, 2009.
- [16] A. J. Scott and M. Grassl. SIC-POVMS: A new computer study. *J. Math. Phys.*, 51:042203, 2010.
- [17] C. Miquel, J. P. Paz, and M. Saraceno. Quantum computers in phase space. *Phys. Rev. A*, 65:062309, 2002.
- [18] M. Nielsen and I. Chuang. *Quantum Computation and Quantum Information*. Cambridge University Press, Cambridge, 2000.
- [19] P. Busch. Informationally complete sets of physical quantities. *Int. J. Theor. Phys.*, 30:1217–1227, 1991.
- [20] H. Weyl. *The Theory of Groups and Quantum Mechanics*. Dover Publications, New York, 1950.
- [21] J. Schwinger. Unitary operator bases. *Proc. Natl. Acad. Sci. U.S.A.*, 46:570, 1960.
- [22] A. Vourdas. Phase space methods for finite quantum systems. *Rep. Math. Phys.*, 40:367–371, 1997.
- [23] A. M. F. Rivas and A. M. Ozorio de Almeida. The Weyl representation on the torus. *Ann. Phys.*, 276:223–256, 1999.
- [24] P. Leboeuf and A. Voros. Chaos-revealing multiplicative representation of quantum eigenstates. *J. Phys. A: Math. Gen.*, 23:1765, 1990.
- [25] S. Nonnenmacher and A. Voros. Chaotic eigenfunctions in phase space. *J. Stat. Phys.*, 92:431–518, 1998.
- [26] I. Bengtsson and K. Życzkowski. *Geometry of quantum states*. Cambridge University press, Cambridge, 2008.
- [27] A. M. Ozorio De Almeida. The Weyl representation in classical and quantum mechanics. *Phys. Rep.*, 295:265–342, 1998.
- [28] V. Bargmann. On a Hilbert space of analytic functions and an associated integral transform Part I. *Comm. Pure App. Math.*, 14:187–214, 1961.
- [29] E. T. Whittaker and G. N. Watson. *A course in modern analysis*. Cambridge University press, Cambridge, 1965.
- [30] <http://www.tandar.cnea.gov.ar/~ermann/sicpovm/>.
- [31] Andreas Klappenecker and M Rotteler. Mutually unbiased bases are complex projective 2-designs. In *Proceedings. International Symposium on Information Theory, 2005. ISIT 2005.*, pages 1740–1744. IEEE, 2005.
- [32] Joseph Emerson, Robert Alicki, and Karol Życzkowski. Scalable noise estimation with random unitary operators. *Journal of Optics B: Quantum and Semiclassical Optics*, 7(10):S347, 2005.
- [33] Christoph Dankert, Richard Cleve, Joseph Emerson, and Etera Livine. Exact and approximate unitary 2-designs and their application to fidelity estimation. *Physical Review A*, 80(1):012304, 2009.
- [34] L. R. Welch. Lower bounds on the maximum correlation of signals. *IEEE Trans. Inf. Theory*, 20:397–399, 1974.
- [35] P. W. Brouwer and C. W. J. Beenakker. Diagrammatic method of integration over the unitary group, with applications to quantum transport in mesoscopic systems. *J. Math. Phys.*, 37:4904–4934, 1996.